

Numerical Analysis of the Power Balance of an Electrical Machine with Rotor Eccentricity

B. Silwal¹, P. Rasilo^{2,1}, L. Perkkiö³, A. Hannukainen³, T. Eirola³, A. Arkkio¹

¹Dept. of Electrical Engineering and Automation, Aalto University, P.O. Box 13000, FI-00076 AALTO, Finland

²Dept. of Electrical Engineering, Tampere University of Technology, P.O. Box 692, FI-33101 TAMPERE, Finland

³Dept. of Mathematics and Systems Analysis, Aalto University, P.O. Box 11100, FI-00076 AALTO, Finland

The power balance in the numerical simulation of a cage induction machine with eccentric rotor has been studied. The asymmetrical air gap flux density distribution caused by the non-uniform air gap due to eccentricity produced forces that play an important role in the rotordynamic stability. These forces act both in the radial and the tangential directions. The tangential force together with the whirling motion produces additional power in the shaft. If the power balance of the simulation satisfies, the power due to the whirling can be calculated from the power balance. This could also give a new approach to compute the forces due to eccentricity or verify the existing force computation methods. The error in the power balance of an eccentric machine has been calculated and the sources of the errors have been illustrated and discussed.

Index Terms— 2-D analysis, Cage induction machine, forces, power balance, rotordynamics, rotor eccentricity, time-stepping finite element method, torque.

I. INTRODUCTION

THE non uniform air gap caused by the eccentricity creates asymmetrical air gap flux density distribution which produces forces, Fig. 1. Rigorous studies have been already done in the past to study the eccentricity, forces and the unbalanced magnetic pull (UMP) caused by the forces [1, 2, 3, 4]. The analytical models have been validated by experimental investigations. Conventionally, there are two types of rotor eccentricity. First, the static eccentricity in which the rotor may be shifted from the center point but does not make any whirling motion. Second, the dynamic eccentricity in which the rotor also makes a whirling motion that is, rotates around the center point at certain frequency and radius called the whirling frequency (ω_w) and the whirling radius respectively. Most of the literature focuses on an eccentric cage induction machine and forces and vibrations related to it. Since the velocity vector of the whirling is also directed towards the direction of the tangential component of the force, they combine to produce a power. This power is very small but plays an important role in the rotordynamics and also in the power balance of the machine. Studies show that the tangential force that mainly contributes to this power changes its direction within a certain frequency range in the vicinity of the whirling frequency and also has a sharp maximum within the same range [1]. This could cause undesired vibrations and

if the natural bending frequency of the shaft somehow falls within this range, even a small power added to the shaft could result into catastrophe. An example of an induction machine failure has been shown in [5]. In this paper we calculate the whirling power and study the power balance of the machine under dynamic eccentricity by including the whirling power. The method based on the power balance has also been used to calculate the torque of an induction machine [6].

If the power balance of an eccentric machine holds at each time step, the power due to the whirling can be calculated from it. This will also give a new approach to verify the force computation methods or even calculate the forces due to eccentricity.

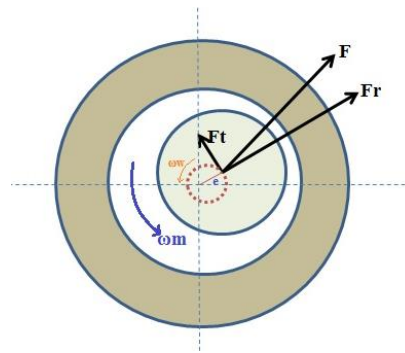


Fig. 1. Forces due to eccentricity. F_r and F_t are the radial and the tangential component of the force respectively

II. METHOD OF ANALYSIS

A. Time-Stepping Finite Element Method

The magnetic field solution is obtained by using a two-dimensional finite element analysis. Time-stepping method based on the magnetic vector potential formulation is used. One period of the fundamental frequency is divided into 600 time steps and second order triangular elements are used for the study. The standard mesh has 4290 elements and 8677 nodes. The magnetic field in the core region of the machine is

Manuscript received April 1, 2015; revised May 15, 2015 and June 1, 2015; accepted July 1, 2015. Date of publication July 10, 2015; date of current version July 31, 2015. (Dates will be inserted by IEEE; “published” is the date the accepted preprint is posted on IEEE Xplore®; “current version” is the date the typeset version is posted on Xplore®). Corresponding author: B. Silwal (email: bishal.silwal@aalto.fi).

Color versions of one or more of the figures in this paper are available online at <http://ieeexplore.ieee.org>.

Digital Object Identifier (inserted by IEEE).

assumed to be two-dimensional. The three dimensional end winding fields are modeled approximately by adding the end-winding impedances to the circuit equations of the windings. The nonlinearity of the materials is taken into account by using the single valued magnetization curve. Trapezoidal rule is used for time integrations.

B. Eccentricity, Forces and Torque

The center position of the rotor is forced to move along a circular path at a constant speed to model the dynamic eccentricity. In addition, the rotor is rotated in its mechanical angular speed. The movement of the rotor is taken into consideration by the moving-band technique.

The forces related to the eccentricity can be calculated by using the Coulomb's method [7] that is based on the principle of virtual work. This method has been chosen over Maxwell stress tensor method because it is considered to be more accurate. The expressions for the force is given by

$$F_{x,y} = \frac{l}{\mu_0} \sum_{e=1}^{N_{\text{seg}}} \int_{\Omega_e} \left[-\mathbf{B}^T \mathbf{G}^{-1} \frac{\partial \mathbf{G}}{\partial x, y} \mathbf{B} + \frac{1}{2} B^2 |\mathbf{G}|^{-1} \frac{\partial |\mathbf{G}|}{\partial x, y} \right] d\Omega, \quad (1)$$

where, N_{seg} is the number of element in the finite element band used in the integration, \mathbf{G} is the Jacobian matrix of the isoparametric mapping, \mathbf{B} is the magnetic flux density.

The same method is used to calculate the torque in this paper. However, the computation of the torque in an eccentric case is difficult. When the torque is integrated over the elements in the air gap of the machine, the radius of integration is important. Generally in FEM, the radius of integration is taken by considering the geometrical center point of the stator as the center which in case of an eccentric machine is not true. Such computation will lead to the torque (T') which is the sum of two components. The first component T_e being the torque corresponding to the whirling radius and the second component T_r which is the real torque acting of the rotor. Therefore, for the accurate calculation of the torque, the effect of the whirling radius should be eliminated. The figurative explanation of this idea is shown in Fig. 2.

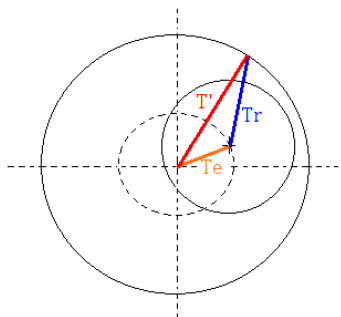


Fig. 2. Torque components corresponding to the radii of integration. The actual torque acting on the rotor is calculated such that $T_r = T' - T_e$

C. Power Balance

The numerical power balance of an electrical machine is studied by using the above-described FEM. The power balance of a normal healthy electrical machine (in motoring

mode) can be given as

$$P_{\text{in}} = P_{\text{loss}} + \frac{dW_f}{dt} + T\omega_m \quad (2)$$

where P_{in} is the input power, P_{loss} is the electromagnetic losses, W_f is the energy of the electromagnetic field and $T\omega_m$ is the power transmitted by the shaft. The powers are calculated as a change in the energy in the given interval of time. The detail of this method can be found in [6]. As mentioned earlier, in case of an eccentric machine where the rotor is whirling, i.e. dynamic eccentricity, the forces together with the velocity vector of the whirling produce a power, which is hereafter in this paper referred to as the whirling power and denoted by P_{whirl} . Therefore, the power balance equation of an eccentric machine should also include the whirling power which can in general be calculated by the dot product of the force and the velocity vector of the whirling. The whirling power and the power balance of an eccentric machine are given as

$$P_{\text{whirl}} = \mathbf{F} \cdot \mathbf{v} \quad (3)$$

$$P_{\text{in}} = P_{\text{loss}} + \frac{dW_f}{dt} + T\omega_m + \mathbf{F} \cdot \mathbf{v} \quad (4)$$

respectively, where \mathbf{F} is the force vector calculated using (1) and \mathbf{v} is the velocity vector of the whirling. The power balance of (4) should hold at any instant of time. If so, the power balance can be used to calculate the forces due to eccentricity by calculating the power due to whirling.

III. RESULTS AND DISCUSSIONS

A 4-pole 15 kW cage induction machine, the parameters of which are given in Table I is used as a test machine in this study. The machine reaches a steady state in a couple of periods of fundamental frequency if the time-stepping simulation is started from a time-harmonic solution as an initial condition. Five periods of 50 Hz frequency are simulated in this paper. The solution of the magnetic field in the cross section of the machine is shown in Fig. 3. The machine was simulated for different values of eccentricity. The forces and the whirling power were calculated. For 20% dynamic eccentricity (whirling radius is equal to 20% of the radial air gap length), the radial and the tangential components of the force as a function of the whirling frequency are shown in Fig. 4. The machine is simulated at the rated slip and voltage. The behavior of the eccentricity harmonics is such that it dampens the forces in all other frequencies expect at some frequencies near the vicinity of the mechanical angular frequency of the rotor. The peaks in the forces in Fig. 4 result from such behavior.

Previous studies have shown that the force increases linearly with the eccentricity. Therefore, the whirling power also increases with the increased level of eccentricity. Fig. 5 shows the whirling power calculated by using (3) for different levels of eccentricity. 0% eccentricity refers to a healthy

machine. The whirling power is very small compared to the rated power of the machine, which is evident from Fig. 5. Therefore, to be able to calculate it from the power balance of the machine, the power balance should be very accurate. The accuracy of the power balance strongly depends on the time integration method used in the simulations. In this study trapezoidal rule is used which is considered to conserve energy well enough to yield results with reasonable accuracy, for instance in a non-linear case. If that is the case, when we substitute the whirling power calculated from (3) into (4) the power balance should hold well enough to give minimum error. Fig. 6 shows the error in the power balance of (4) in that case.

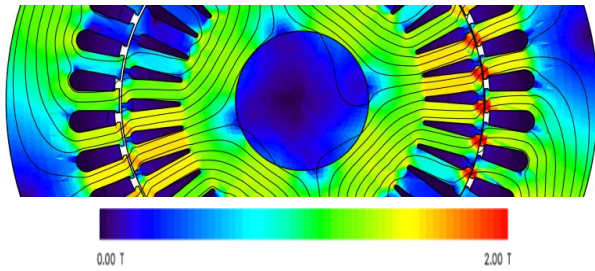


Fig. 3. Flux density distribution in an eccentric machine cross-section

TABLE I
TEST MACHINE PARAMETERS

Parameter	Value
Number of poles	4
Connection	Delta
Rated Voltage [V]	380
Supply frequency [Hz]	50
Rated Current [A]	31
Rated Power [kW]	15

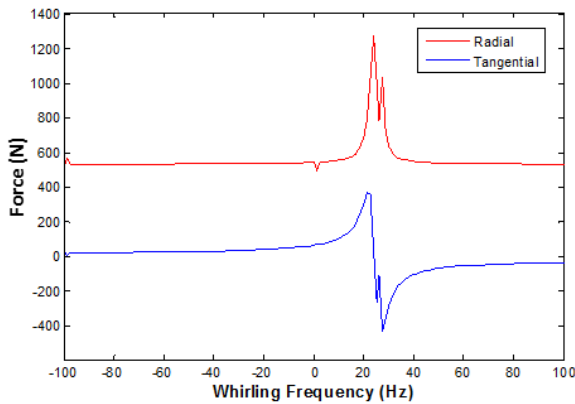


Fig. 4. Eccentricity forces as a function of whirling frequency. The tangential force changes direction within some range of frequency

The results suggest that in a healthy machine the power balance is well satisfied but when the whirling power is added, the error increases. As the whirling power increases with eccentricity, an increasing trend is seen in the error as well. Now, the important question is- what are the possible sources

of errors? One source of error is the third term in the Right Hand Side (RHS) of (4). Previous studies have shown that the accurate computation of the torque is very much dependent on the type of finite element discretization used in the air gap of the machine [6]. The shape and the uniformity of the elements also affect the computation and in case of an eccentric machine where the air gap is non-uniform, it is inevitable. Fig. 7 shows the average torque and the corresponding error in the power balance calculated for five different types of mesh in the air gap of the machine, with 33% eccentricity. In this study, as different discretizations were used of the air gap of the machine, the total number of the nodes and elements vary from the numbers mentioned in previous section. The results describe well the sensitivity of the torque and thus the error in the power balance with respect to the type of mesh used. Even though the change in the torque values seems much smaller, it makes a significant effect relative to the magnitude of the whirling power. For instance, the difference between the maximum and the minimum torque among the five cases studied is 0.121 Nm. The corresponding power related to this difference is 18.4 W, which is significant in this case.

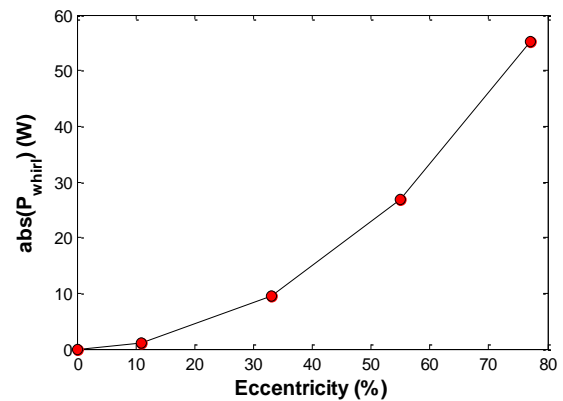


Fig. 5. Power produced due to the whirling as a function of the eccentricity

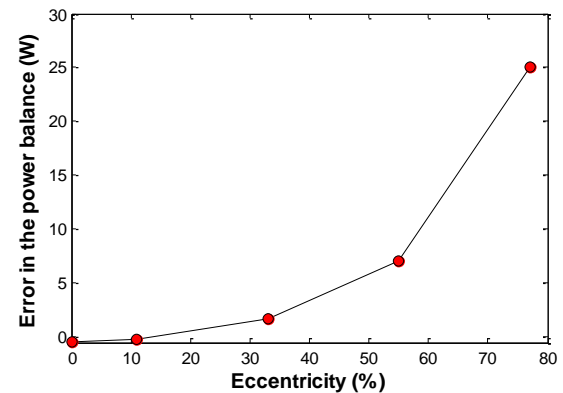


Fig. 6. The error in the power balance of the machine as a function of eccentricity

The re-meshing done to model the rotation of the rotor also adds some error in the power balance. This can be well illustrated by comparing two cases. In the first case, the rotor is rotating at its rated speed and the rotation is modeled by re-meshing and the second case, the rotor is locked. The errors in the power balance in such cases are shown in Fig. 8. It can be

clearly seen that the error in the locked rotor case does not change much with an increasing eccentricity whereas the error in the case when rotation is included rises. In the locked rotor case, the third term in the RHS of (5) is zero. This suggests that the error in the power balance mainly comes from the type of mesh used and the re-meshing which actually affects the third term in the RHS of (5), thus affecting the power balance. The situation gets worse in case of dynamic eccentricity because in this case, in addition to the re-meshing the rotor mesh is also moved in a circular orbit around the geometrical centerline of the stator. This adds to the non-uniformity of the mesh in the air gap, which contribute more error. This can be explained by a study similar to the one above but without whirling (static eccentricity). Fig. 9 shows the error in the power balance in both dynamic and static eccentricity cases when the machine is at rated speed. Comparison of the errors makes it clear that the whirling itself adds more error in the power balance by making the mesh in the air gap non-uniform. The non-uniformity increases with the level of the eccentricity and so is the difference between the errors.

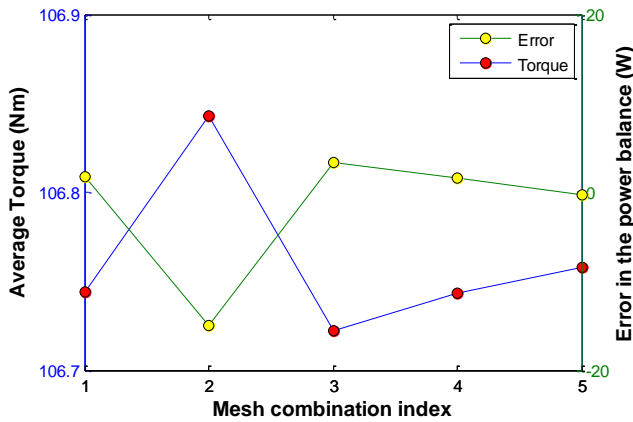


Fig. 7. The average torque calculated with different 5 different types of mesh in the air gap and the corresponding error in the power balance. It is clear that the error is sensitive to the type of mesh used. Mesh Index: XYZ, X=Number of layers, Y = Movement layer, Z=Torque computation layer; 1=111, 2=221, 3=222, 4=321, 5=332

IV. CONCLUSION

The power balance of an eccentric machine has been studied using finite element method. The small power produced due to the whirling has been included in the power balance. The error in the power balance has been calculated and the possible sources of the errors are described and discussed. It is seen that that error in the torque related to the type of mesh in the air gap and the re-meshing lead to large error in the power balance. Other than the mesh, the time integration method should be investigated more in order to find more sources of errors. In this paper, trapezoidal rule is used. Some higher order time integration method could be tested to ensure more accuracy. This paper also briefly highlights an accurate method to calculate the torque of a machine when the rotor is eccentric.

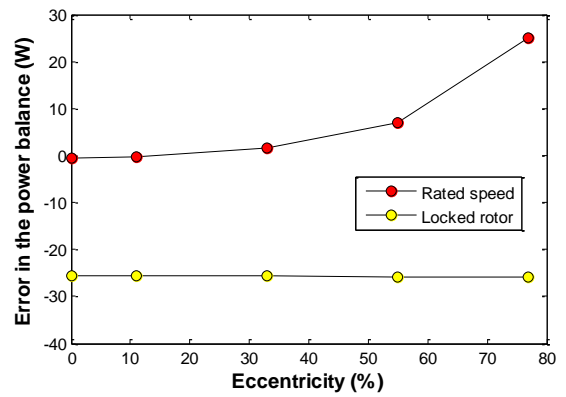


Fig. 8. Power balance error in the case of dynamic eccentricity

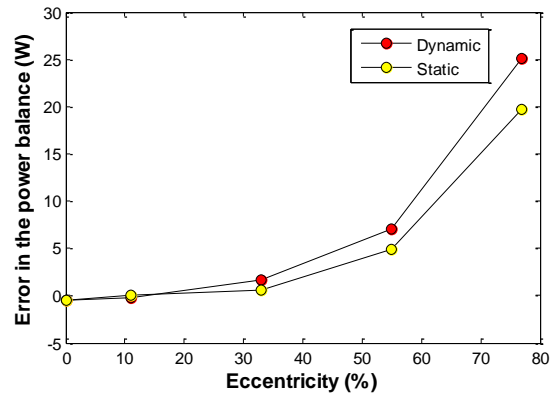


Fig. 9. Power balance error in the case of both dynamic and static eccentricity, simulated at rated speed. In the static eccentricity case, there is no whirling and the power related to it.

ACKNOWLEDGMENT

This work was supported by the Academy of Finland, Helsinki.

REFERENCES

- [1] A. Arkkio, M. Antila, K. Pokki, A. Simon, E. Lantto, "Electromagnetic force on a whirling cage rotor," *IEE Proc. Elect. Power Appl.*, vol. 147, no. 5, pp. 353-360, Sept. 2000.
- [2] A. C. Smith, D. G. Dorrell, "Calculation and measurement of unbalanced magnetic pull in cage induction motors with eccentric rotors. I. Analytical model," *IEE Proc. Elect. Power Appl.*, vol. 143, no. 3, pp. 193-201, May 1996.
- [3] D. G. Dorrell, A. C. Smith, "Calculation and measurement of unbalanced magnetic pull in cage induction motors with eccentric rotors. II. Experimental investigation," *IEE Proc. Elect. Power Appl.*, vol. 143, no. 3, pp. 202-210, May 1996.
- [4] L. Wang, R. W. Cheung, Z. Ma, J. Ruan, Y. Peng, "Finite-element analysis of unbalanced magnetic pull in a large hydro-generator under practical operations," *IEEE Trans. Magn.*, vol. 44, no. 6, pp. 1558-1561, June 2008.
- [5] J. Hong, D. Hyun, S. B. Lee, C. Kral, "Offline monitoring of airgap eccentricity for inverter-fed induction motors based on the differential inductance," *IEEE Trans. Industry Appl.*, vol. 49, no. 6, pp. 2533-2542, Nov-Dec. 2013.
- [6] B. Silwal, P. Rasilo, L. Perkkiö, M. Oksman, A. Hannukainen, T. Eirola, A. Arkkio, "Computation of torque of an electrical machine with different types of finite element mesh in the air gap" *IEEE Trans. Magn.*, vol. 50, no. 12, pp. 1-9, Dec. 2014.
- [7] J. L. Coulomb, "A methodology for the determination of global electromechanical quantities from a finite element analysis and its application to the evaluation of magnetic forces, torques and stiffness," *IEEE Trans. Magn.*, vol. 19, no. 6, pp. 2514-2519, Nov. 1983.